[American Journal of Science, Vol. 311, January, 2011, P. 63–75, DOI 10.2475/01.2011.03]

DECLINING ATMOSPHERIC CO_2 DURING THE LATE MIDDLE EOCENE CLIMATE TRANSITION

GABRIELA DORIA*,**, DANA L. ROYER*,†, ALEXANDER P. WOLFE***, ANDREW FOX§, JOHN A. WESTGATE§§, and DAVID J. BEERLING§

ABSTRACT. The transition from the extreme greenhouse of the early Paleogene (~52 Ma) to the present-day icehouse is the most prominent change in Earth's Cenozoic climate history. During the late Middle Eocene climate transition (42-38 Ma), which preceded the onset of long-lived, continental-scale ice sheets, there is concordant evidence for brief pulses (<1 m.y. in length) of global warmth and ice sheet growth but few constraints on atmospheric CO_2. Here we estimate the concentration of atmospheric CO_2 during this critical interval using stomatal indices of fossil *Metasequoia* needles from ten levels in an exceptionally well-preserved core from the Giraffe kimberlite locality in northwestern Canada. Reconstructed CO_2 concentrations are mainly between 700 to 1000 ppm, but include a secular decline to 450 ppm towards the top of the investigated section. Because the CO_2 threshold for nucleating continental ice sheets at this time was ~500 to 750 ppm, the CO_2 decline is compatible with a rapid ($<10^4$ yrs) transition from warm, largely ice-free conditions to cooler climates with ice sheets. These fossils provide direct evidence that high-latitude deciduous forests thrived in the geological past under CO_2 concentrations that will likely be reached within the 21st century (500-1000 ppm).

Key words: Paleoclimate, carbon dioxide, stomata, Eocene, kimberlite, *Metasequoia*

INTRODUCTION

Paleotemperature (Zachos and others, 2001; Tripati and others, 2005; Edgar and others, 2007; Burgess and others, 2008; Bohaty and others, 2009; Eldrett and others, 2009) and glacial sediment (Ehrmann and Mackensen, 1992; Eldrett and others, 2007; St. John, 2008; Tripati and others, 2008; Stickley and others, 2009) records demonstrate that the inception of the current icehouse climate mode was not strictly coincident with the Eocene-Oligocene boundary (33.9 Ma); instead, the Earth "staggered" into the boundary, punctuated by short-lived (<1 m.y.) warm and cool phases (fig. 1). The best documentation of these climate flickers come from the late Middle Eocene climate transition (42-38 Ma). Multiple studies report a warm phase from ~41.9 to 41.7 Ma (Edgar and others, 2007; Burgess and others, 2008), followed by sharp cooling and ice sheet growth from ~41.6 to 40.6 Ma (Tripati and others, 2005; Edgar and others, 2007; Bohaty and others, 2009; Eldrett and others, 2009). Another warm phase ensued from 40.4 to 39.9 Ma (the Middle Eocene climatic optimum, MECO) (Bohaty and Zachos, 2003; Ivany and others, 2008; Bohaty and others, 2009), followed immediately by cooling and ice sheet growth (Tripati and others, 2005; Eldrett and others, 2009) (fig. 1). Together, these records suggest a pattern of repeated, rapid ($<10^5$ yrs) climate excursions during the late Middle Eocene. However, very little is known about atmospheric CO_2 during this time (Pagani and others,

* Department of Earth and Environmental Sciences, Wesleyan University, Middletown, Connecticut 06459, USA
** Present address: School of Forestry and Environmental Studies, Yale University, New Haven, Connecticut 06511, USA
*** Department of Earth and Atmospheric Sciences, University of Alberta, Edmonton, Alberta T6G 2E3, Canada
§ Department of Animal and Plant Sciences, University of Sheffield, Sheffield S10 2TN, United Kingdom
§§ Department of Geology, University of Toronto, Toronto, Ontario M5S 3B1, Canada
† Corresponding author: droyer@wesleyan.edu

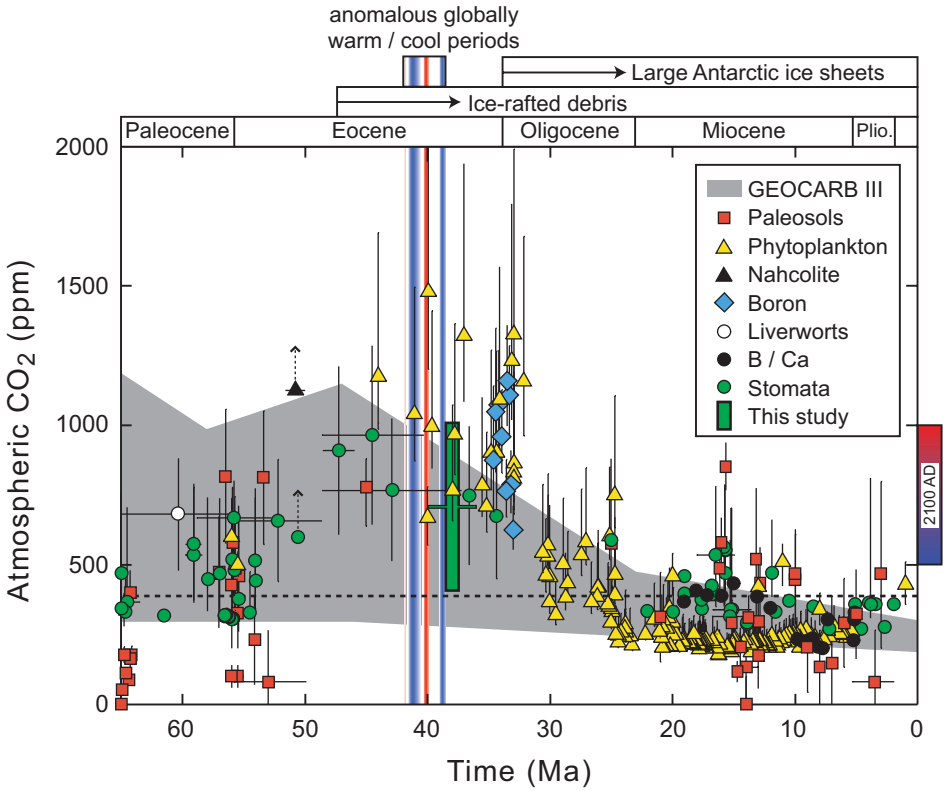

Fig. 1. Cenozoic evolution of CO_2. Estimates of atmospheric CO_2 are from proxies and a long-term carbon cycle model (GEOCARB III; Berner and Kothavala, 2001). The vertical green rectangle represents the range of CO_2 estimates presented here (compare with fig. 5B). The thin, vertical red and blue stripes correspond to anomalous warm and cool periods that are thought to be global (see INTRODUCTION). The temporal range of ice-rafted debris in the northern (Eldrett and others, 2007; St. John, 2008; Tripati and others, 2008; Stickley and others, 2009) and southern (Ehrmann and Mackensen, 1992) hemispheres, and the onset of large, long-lived ice sheets on Antarctica (Zachos and others, 2001) are noted along the top. Also noted along the right-hand axis is the range of predicted atmospheric CO_2 concentrations for 2100 AD (IPCC, 2007). For context, the horizontal dashed line represents the annually-integrated CO_2 concentration for 2009 AD at Mauna Loa, Hawaii (387 ppm) (Keeling and others, 2009). The paleosol carbonate (Cerling, 1992; Koch and others, 1992; Sinha and Stott, 1994; Ekart and others, 1999; Royer and others, 2001b; Nordt and others, 2002, 2003; Retallack, 2009b), phytoplankton (Freeman and Hayes, 1992; Stott, 1992; Pagani and others, 2005b), and stomatal (Kürschner and others, 1996, 2001, 2008; Retallack, 2001, 2009a; Royer and others, 2001b; Beerling and others, 2002; Greenwood and others, 2003; Royer, 2003; Smith and others, 2010) methods are the most robust and commonly-used paleo-CO_2 proxies (Royer and others, 2001a). The B/Ca (Tripati and others, 2009) and liverwort (Fletcher and others, 2008) methods are also included. The presence of nahcolite in the Green River Formation at 50.5 Ma places a basement CO_2 value of 1125 ppm (Lowenstein and Demicco, 2006); new mineral equilibria experiments suggest that this basement value may need to be revised downward (Jagniecki and others, 2010). The boron method is not reliable for pre-Pleistocene estimates (Lemarchand and others, 2000; Royer and others, 2001a; Pagani and others, 2005a; Klochko and others, 2006, 2009), although the study of Pearson and others (2009) is the first to address some of the concerns and is included here. Paleosol carbonate CO_2 estimates have been adjusted to reflect a soil CO_2 concentration of 2000 ppm (Breecker and others, 2009). Estimates from the goethite proxy (Yapp and Poths, 1996; Yapp, 2004; Tabor and Yapp, 2005; Feng and Yapp, 2009) are excluded due to poor knowledge of some of the isotopic fractionation factors (Rustad and Zarzycki, 2008). For Retallack (2009a), only data points associated with >4 cuticle fragments are included (Royer, 2003) and the stomatal ratio approach (Beerling and Royer, 2002) is used to estimate CO_2 for species other than *Ginkgo adiantoides*. Estimates from Royer and others (2001b) and Royer (2003) have been updated by Beerling and others (2009). All dates are calibrated to the timescale of Gradstein and others (2004).

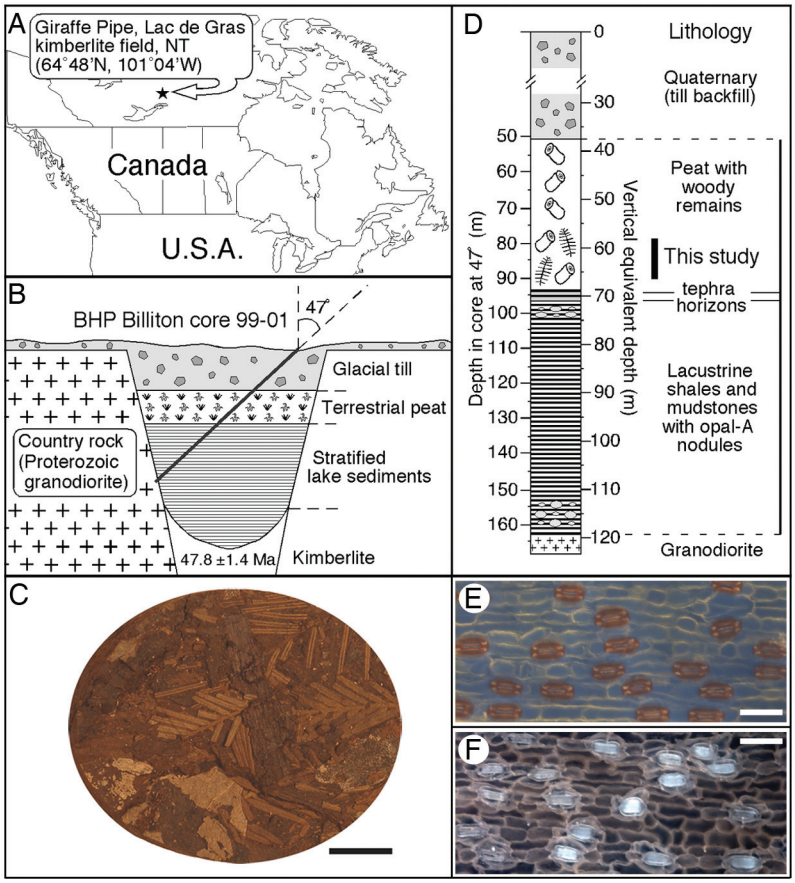

Fig. 2. Giraffe kimberlite locality and *Metasequoia* leaves. (A) Map of region. (B) Schematic stratigraphy of posteruptive sediments in the kimberlite diatreme. (C) Bedding plane of Giraffe core showing mummified *M. occidentalis* leaves (scale bar = 1 cm). (D) Lithostratigraphy and chronology of sediments considered here. (E) Abaxial leaf cuticle of extant *M. glyptostroboides*. (F) Abaxial leaf cuticle of fossil *M. occidentalis* from Giraffe locality. E–F, epifluorescence microscopy (scale bars = 50 μm).

2005b; Royer, 2006) (fig. 1). In particular, high-resolution records from individual proxies are lacking, which limits a basic understanding of the paleoclimate system.

SEDIMENTARY ARCHIVE FROM A KIMBERLITE PIPE

We exploited the availability of well-preserved fossil *Metasequoia* foliage in a sediment core from the Giraffe kimberlite pipe in northern Canada (~62 °N paleolatitude; Torsvik and others, 2001, 2008) to improve constraints on the atmospheric CO_2 regime during the late Middle Eocene climate transition. The Giraffe site contains late Middle Eocene lacustrine and terrestrial sediments capped by Pleistocene glacial till and underlain by kimberlite emplaced 47.8 ± 1.4 Ma (Wolfe and others, 2006) (fig. 2). The core contains 32.7 m of peat with abundant wood and foliage, underlain by 51.1 m of stratified lacustrine mudstone; these thicknesses include correction for the 47° drilling angle. The depositional environment of the peat is interpreted as an infilled maar crater with the immediate vicinity dominated by *Metasequoia* forests (Wolfe and others, 2006).

The Giraffe peat today is ~360 m a.s.l. and elevation of the peat during the late Middle Eocene was probably ≤360 m a.s.l. This is because the protracted regional stability of the Slave Craton, into which the Giraffe kimberlite intruded, has resulted in near-zero diagenetic alteration of the fossil content, as testified by the outstanding preservation of the fossil remains, and by thermal maturation of the material (only slightly greater than that of modern peat) (Wolfe and others, 2006). Tectonic stability in this region is also supported by the lack of either post-Eocene faulting or Pleistocene glaciotectonism. Because of the low inferred paleoelevation for the Giraffe locality, we assumed equivalency between CO_2 partial pressure (Pa) and mole fraction (ppm) (Beerling and Royer, 2002).

The age of the peat is constrained by three fission-track dates from two calc-alkaline rhyolitic tephra beds at the base of the peat (fig. 2; Wolfe and others, 2006) using both diameter-corrected ($n = 2$) and isothermal-plateau ($n = 1$) techniques (Westgate and others, 2006), which produce a weighted-mean age model of 37.84 ± 1.99 Ma. Our studied peat section (7.54 m) represents ~10^4 yrs assuming a similar accumulation rate as the peat-to-lignite grade, Middle Eocene *Metasequoia* swamp deposits at Napartulik on Axel Heiberg Island, Canada (~1 mm/yr) (Greenwood and Basinger, 1993; Kojima and others, 1998); for comparison, accumulation rates in uncompacted, submodern peat rarely exceed 10 mm/yr (for example, Goslar and others, 2005). The unusual physical setting of Giraffe, along with post-eruptive tectonic and thermal stability, has resulted in exceptional, Lagerstätte-quality preservation of both aquatic (Wolfe and others, 2006) and terrestrial fossils (fig. 2). This provides an opportunity to study, with very high temporal resolution, the evolution of a pre-Pleistocene terrestrial ecosystem.

THE STOMATAL APPROACH FOR RECONSTRUCTING PALEO-CO_2

The dominant foliage at Giraffe is *Metasequoia occidentalis* (Newberry) Chaney (fig. 2), a long-ranging taxon (Late Cretaceous to Pleistocene) that is probably conspecific with extant *M. glyptostroboides* Hu and Cheng based on similarity in morphology (LePage and others, 2005; Liu and Basinger, 2009), biochemistry (Yang and others, 2005), and inferred physiology (Vann, 2005). Here we use the fossil record of isolated cuticles from fossil *M. occidentalis* needles to develop a record of stomatal index (SI, the fraction of epidermal cells that are stomata) (Salisbury, 1927) for estimating paleo-CO_2 concentrations during the late Middle Eocene. The stomatal method for quantitative paleo-CO_2 estimation is based on the species-specific, nonlinear inverse relationship between atmospheric CO_2 partial pressure and SI (Woodward and Bazzaz, 1988; Royer, 2001). The technique is underpinned by well-defined genetic (Gray and others, 2000; Casson and Gray, 2008), functional (Wynn, 2003; Kleidon, 2007; Konrad and others, 2008), and systemic signaling (Lake and others, 2001, 2002) pathways allowing leaves to respond to atmospheric CO_2 change. It has yielded multiple Pleistocene and Holocene CO_2 reconstructions that are verified against ice core CO_2 records (Rundgren and Beerling, 1999, 2003; McElwain and others, 2002; Rundgren and others, 2005). Cross-species comparisons for the mid-Miocene (~15 Ma) indicate similar CO_2 estimates from fossil *M. occidentalis* to those from coeval *Ginkgo* cuticles and other CO_2 proxies (Royer and others, 2001b). A central advantage of adopting SI rather than any other measure of stomatal abundance or geometry is its relative insensitivity to water stress which affects epidermal cell size, and therefore stomatal density, but not the conversion of epidermal cells to stomata controlling SI (Salisbury, 1927; Kürschner, 1997; Royer, 2001; Sun and others, 2003).

METHODS

The Eocene fossil history of *Metasequoia* SI was calibrated by extending an earlier dataset (Royer and others, 2001b) with new information from field-grown *M. glyptostrobo-*

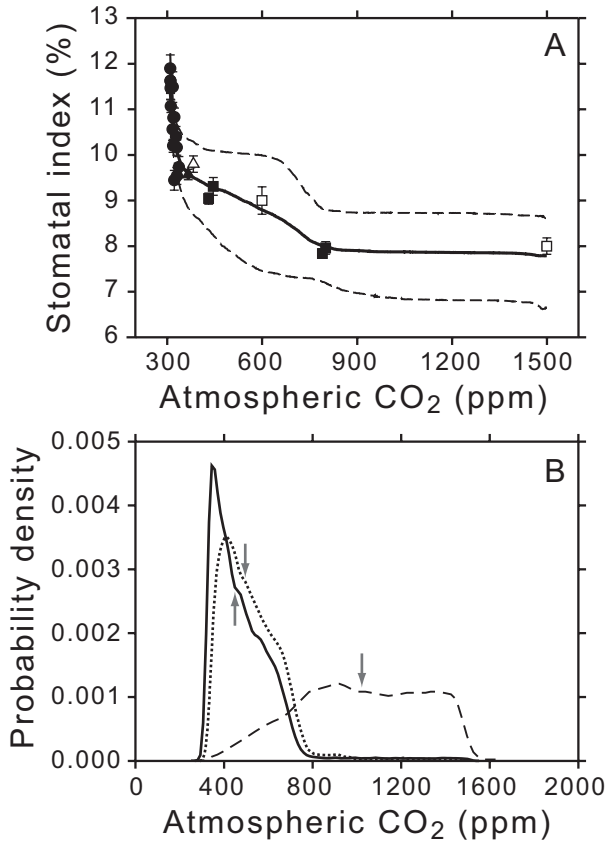

Fig. 3. Response of stomatal index (SI) to atmospheric CO_2 in *Metasequoia glyptostroboides*. (A) Calibration between SI and atmospheric CO_2. Data presented here (open symbols) are combined with a previously published calibration (filled symbols) (Royer and others, 2001b). Leaves come from dated herbaria sheets (circles), field-grown trees (triangles), and growth chamber experiments (squares). Error bars: ±1 s.e.m. Solid line: median Monte Carlo simulation (Beerling and others, 2009); dashed lines: 5 and 95 percentiles of 2000 functions fitted to pseudo-datasets. (B) Examples of probability density functions for estimates of atmospheric CO_2 from fossil *Metasequoia*. Solid line: mean SI = 9.85%; depth = 58.16 m. Short dashed line: mean SI = 9.29%; depth = 58.50 m. Long dashed line: mean SI = 7.73%; depth = 59.24 m; the truncation around 1500 ppm is an artifact of the calibration data (see calibration section for discussion). Gray arrows denote median CO_2 estimates.

ides trees experiencing present-day CO_2 concentration (384 ppm, *circa* 2007 AD) (Keeling and others, 2009), and young saplings grown in controlled environments at ambient and elevated CO_2 concentrations (600 and 1500 ppm) (fig. 3). Eight two-year old saplings were used for all measurements (Broken Arrow Nursery; Hamden, Connecticut, USA). First, fully-expanded leaves were sampled (384 ppm treatment). Plants were then randomly divided and placed into one of two independently-controlled growth chambers (Conviron CMP-5090; Winnipeg, Manitoba, Canada). Environmental conditions in the chambers were identical except for CO_2 concentration (600 and 1500 ppm treatments). A 16 hour day length was simulated (440-600 $\mu mol\ m^{-2}\ s^{-1}$ irradiance, depending on height within canopy), with temperature linearly increasing from 19 °C to 25 °C over 8 hours and then declining in a similar fashion to 19 °C. Relative humidity was fixed at 75 percent.

For extant leaves, five fully-expanded leaves from each plant were collected from the outer portions of the canopies at a uniform height. For plants growing at high CO_2

(600 and 1500 ppm), harvesting occurred after six months of growth in the chambers and only leaves whose buds had developed in the experimental conditions were selected. For fossil leaves, five complete needles or needle fragments were sampled from each of 10 depths between 58.16 and 65.70 m in the Giraffe core (fig. 2).

A two-step maceration method was used to isolate the leaf cuticles. Leaves were first submerged in 70 percent nitric acid for one hour or until the leaf segments turned yellowish-brown. Cuticles were then rinsed three times with distilled water and submerged in 30 percent aqueous chromium trioxide for 48 hours. Cuticles were again rinsed and then, for extant leaves, stained with Safranin-O aqueous solution (0.25% m/v).

Cuticles were mounted dry for epifluorescence microscopy (420-490 nm filter) or in glycerol for transmitted light microscopy (Leica DMBL; Leica Microsystems). For each leaf, we measured the number of stomatal complexes (stomatal pore + bounding guard cells) and number of epidermal cells (including subsidiary cells) for four fields-of-view from the middle third (when available) of the abaxial surface of the needle. Non-stomatal areas along the midvein and leaf margin were avoided. For each field-of-view of the extant leaves, the guard cell length for ten stomatal complexes was also measured. All fields-of-view (0.1336 mm^2) were photographed with a Leica DFC300FX digital camera and analyzed using Image-pro Plus software (v. 5.1; MediaCybernetics). The unit of replication for all statistics associated with experiments is the plant ($n = 4$ per CO_2 treatment), and with fossils is the leaf ($n = 5$ per level).

Our calibration (fig. 3A) is the most extensive for any plant lineage and was used in a new Monte Carlo-type simulation approach to develop a twice differentiated monotonic function describing the SI-CO_2 relationship that incorporates uncertainties in training set measurements and curve fitting procedures (Beerling and others, 2009). Atmospheric CO_2 concentrations were estimated 500 times for each SI value by inversion of the SI-CO_2 function using Monte Carlo simulations and assuming Gaussian error distribution for the SI error term; kernel density estimates of the probability density functions were then constructed from the results (Beerling and others, 2009) (fig. 3B). Low SI values produce more uncertain CO_2 estimates because they are in the less sensitive part of the calibration function (fig. 3A; for full discussion, see Beerling and others, 2009). Because the variance of fossil SI also affects estimated paleo-CO_2, reconstructed CO_2 values are not always strictly inversely proportional to SI. For example, a bed may have a higher reconstructed CO_2 value compared to another bed with a slightly lower SI if its variance is large.

Metasequoia leaves from Giraffe were also prepared for stable carbon isotopic ($\delta^{13}C$) analysis. Whole *Metasequoia* leaf samples from each level (where sufficient numbers were available) were treated with 30 percent HCl for 24 h and rinsed several times in distilled water to remove carbonates prior to oven drying at 70 °C for 48 h. $\delta^{13}C$ measurements were made in triplicate on oven-dried, ground fossil needles with an isotopic ratio mass spectrometer (ANCA GSL preparation module, 20-20 stable isotope analyser, PDZ Europa, Cheshire, UK).

CALIBRATION OF METASQUOIA AND MIDDLE EOCENE RECORD OF CO_2

In our experiments, *Metasequoia* shows a significant decline in SI with rising CO_2 (fig. 4A; $F_{(2,77)} = 15.6$, $P < 0.001$, one-way ANOVA). This nonlinear relationship is similar to that observed in previous calibrations (fig. 3A), providing strong support for the sensitivity of stomatal development to CO_2 in *Metasequoia*.

Stomatal index is typically independent of stomatal size. It is possible that stomatal pore area per leaf area may reflect a closer functional relationship with atmospheric CO_2. However, stomatal pore index, calculated as stomatal density × the square of guard cell length (Sack and others, 2003), is invariant across our three CO_2 treatments (fig. 4A; $F_{(2,77)} = 0.005$, $P = 0.995$, one-way ANOVA). This invariance is due to the

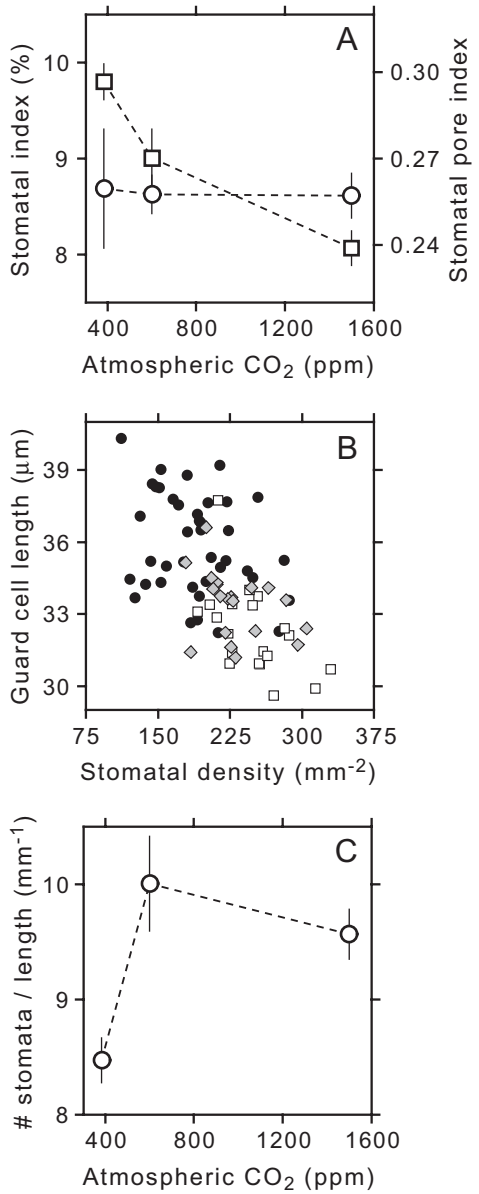

Fig. 4. Relationships in calibration data between atmospheric CO_2 and stomatal dimensions. (A) CO_2 vs. stomatal index (squares; compare with open symbols in fig. 3A) and stomatal pore index (circles). Error bars, ±1 s.e.m. (B) Inverse covariation between stomatal density and pore size. Symbols correspond to the three experiments: 384 ppm CO_2 (circles), 600 ppm CO_2 (squares) and 1500 ppm CO_2 (diamonds). Unit of replication is leaves. (C) CO_2 vs. stomatal number per length. Error bars, ±1 s.e.m.

inverse covariation between stomatal density and stomatal size (fig. 4B) (Hetherington and Woodward, 2003; Franks and Beerling, 2009).

In some conifers, stomatal density and index are not considered appropriate CO_2 proxies because of the regular arrangement of their stomata into rows; instead, measurements related to stomatal number per length are advocated (Kouwenberg and

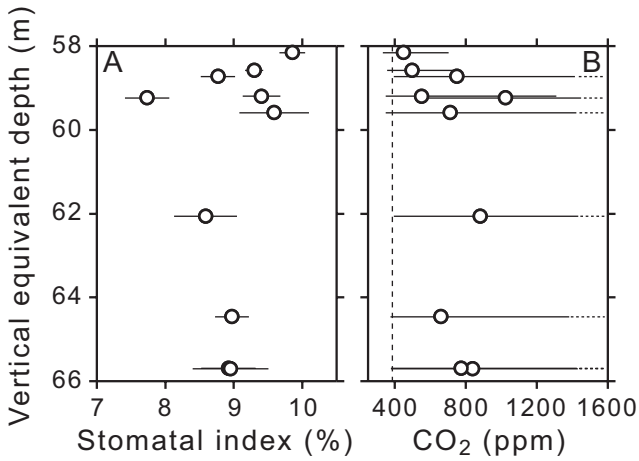

Fig. 5. CO_2 record from Giraffe fossil locality. (A) Stomatal index of fossil *Metasequoia* leaves. Error bars: ±1 s.e.m. (B) Estimated median atmospheric CO_2 concentration from stomatal index using a Monte Carlo simulation (Beerling and others, 2009). Error bars: 5 and 95 percentiles of 2000 functions fitted to pseudo-datasets; horizontal dashed lines denote poorly-constrained upper limits (see calibration section for discussion). Vertical dashed line represents the annually-integrated CO_2 concentration for 2009 AD at Mauna Loa, Hawaii (387 ppm) (Keeling and others, 2009).

others, 2003). However, stomatal number per length did not inversely relate to CO_2 in our experiments (fig. 4C). Further, stomatal rows in *Metasequoia* are only semi-ordered (figs. 2E-F), making such measurements highly irreproducible. In summary, SI is the most appropriate stomatal measure for reconstructing paleo-CO_2 in *Metasequoia*.

At Giraffe, reconstructed atmospheric CO_2 concentrations range between ~700 to 1000 ppm for the bottom ~90 percent of the studied core (mean 5 and 95% percentiles = −378 and +636 ppm), before dropping sharply to 450 ppm towards the core top (mean 5 and 95% percentiles = −128 and +243 ppm) (fig. 5). Critically, the CO_2 drop from the lowermost eight levels in the core to the topmost two levels is statistically significant ($P = 0.03$, one-tailed z-test; within- and between-level variance combined by quadrature). The influence of water availability on our CO_2 reconstruction was likely minimal because the $\delta^{13}C$ of the leaves, a sensitive indicator of water availability (Farquhar and others, 1989), lacks covariance with stomatal density or SI (fig. 6).

We note that the mean SI at one level (59.24 m) is lower than what is captured in our calibration (compare fig. 3A with fig. 5A); as a result, the reconstructed CO_2 for this level is likely a minimum, with the upper limit poorly constrained. Similarly, the upper CO_2 constraints at several other levels are uncertain because their SI's are near the flat portion of the calibration (<8.7%). These caveats are important for a general understanding of paleo-CO_2 estimates from fossil leaves (Beerling and others, 2009; Smith and others, 2010); within the specific context of the current study, the caveats imply that we may have underestimated the magnitude of CO_2 decline through our section.

IMPLICATIONS FOR ICE AND HIGH-LATITUDE DECIDUOUS FORESTS

The CO_2 history from Giraffe agrees broadly with coeval estimates from other proxies and from geochemical modeling of the long-term carbon cycle (fig. 1). Collectively, atmospheric CO_2 estimates from the leading CO_2 proxies (IPCC, 2007) indicate values ~300 to 800 ppm during the Paleocene and early Eocene, rising to

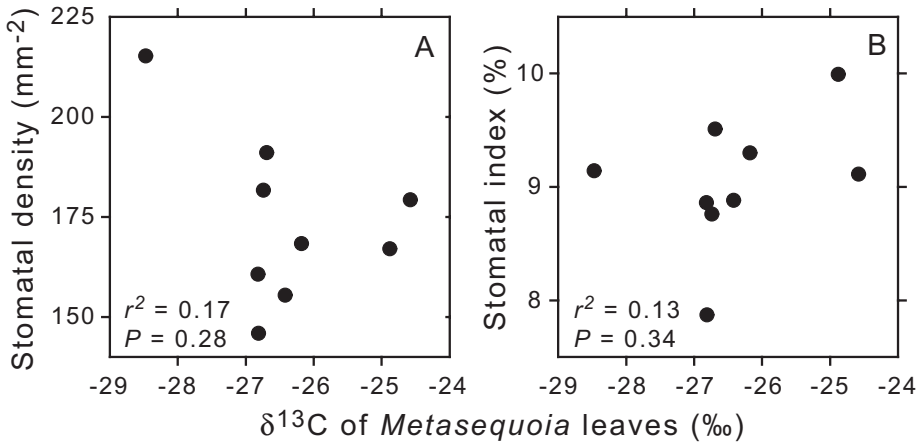

Fig. 6. Relationship between the $\delta^{13}C$ of fossil *Metasequoia* leaves and their (A) stomatal index and (B) stomatal density. In both cases, the least-squares linear regression is not significant, suggesting that any potential water availability gradients in the Giraffe core did not significantly impact stomatal distributions in *Metasequoia* (see main text).

~700 to 1300 ppm during the remainder of the Eocene (fig. 1). Atmospheric CO_2 then declined towards values mostly <500 ppm with the onset of large-scale glaciation on Antarctica. Uncertainty in the absolute age control on our sequence precludes establishing a precise link between CO_2 and a single temperature excursion such as the MECO event (fig. 1). However, geological records (Pagani and others, 2005b; Royer, 2006; Pearson and others, 2009; Peters and others, 2010) and climate models (DeConto and Pollard, 2003; Pollard and DeConto, 2005; DeConto and others, 2008) support a CO_2 threshold for triggering ice sheet growth during the mid-Cenozoic of ~500 to 750 ppm. Atmospheric CO_2 reconstructed from the Giraffe core spans this threshold, with the decline towards the core top being consistent with a rapid ($<10^4$ yrs) transition from a largely ice-free Earth to one with at least some continental ice sheets. The tempo of our observed CO_2 drop broadly matches the tempo of observed temperature changes during the Middle Eocene climate transition (~10^5 yrs; see INTRODUCTION).

Our CO_2 reconstruction is the first to be derived from sediments that also provide direct evidence for high-latitude deciduous forests. Our study highlights the possibility that productive, high-latitude forest ecosystems were maintained under modestly elevated CO_2 concentrations given a long-term ($>10^3$ yrs) climate system response. Continued anthropogenic CO_2 emissions are raising Earth's CO_2 concentration towards the lower limit of CO_2 envelope reconstructed here (450 ppm) and will undoubtedly exceed it in the near future (IPCC, 2007). Observations at the northern limit of boreal forests indicate that migration of trees and shrubs into arctic tundra is already occurring (Sturm and others, 2001; Lloyd, 2005). Human-induced environmental change has the potential to reinstate boundary conditions comparable to those under which long-extinct polar deciduous forests arose.

ACKNOWLEDGMENTS

We thank BHP Billiton Diamond Inc. and the Geological Survey of Canada (Calgary) for archiving material, David Wilton for technical support, Ben Palmer for isotopic determinations of the fossil needles, Gary Upchurch for advice about cuticle preparation, and Ben LePage, Barry Chernoff, and Fernando Vargas for helpful

discussions. We thank two anonymous reviewers whose comments helped improve the manuscript. A.P.W. and J.A.W. were supported by the Natural Sciences and Engineering Research Council of Canada. D.J.B. gratefully acknowledges funding from the Leverhulme Trust and through a Royal Society-Wolfson Research Merit Award.

References

Beerling, D. J., and Royer, D. L., 2002, Fossil plants as indicators of the Phanerozoic global carbon cycle: Annual Review of Earth and Planetary Sciences, v. 30, p. 527–556, doi: 10.1146/annurev.earth.30.091201.141413.

Beerling, D. J., Lomax, B. H., Royer, D. L., Upchurch, G. R., Jr., and Kump, L. R., 2002, An atmospheric pCO_2 reconstruction across the Cretaceous-Tertiary boundary from leaf megafossils: Proceedings of the National Academy of Sciences of the United States of America, v. 99, p. 7836–7840, doi: 10.1073/pnas.122573099.

Beerling, D. J., Fox, A., and Anderson, C. W., 2009, Quantitative uncertainty analyses of ancient atmospheric CO_2 estimates from fossil leaves: American Journal of Science, v. 309, p. 775–787, doi: 10.2475/09.2009.01.

Berner, R. A., and Kothavala, Z., 2001, GEOCARB III: A revised model of atmospheric CO_2 over Phanerozoic time: American Journal of Science, v. 301, p. 182–204, doi: 10.2475/ajs.301.2.182.

Bohaty, S. M., and Zachos, J. C., 2003, Significant Southern Ocean warming event in the late Middle Eocene: Geology, v. 31, p. 1017–1020, doi: 10.1130/G19800.1.

Bohaty, S. M., Zachos, J. C., Florindo, F., and Delaney, M. L., 2009, Coupled greenhouse warming and deep-sea acidification in the middle Eocene: Paleoceanography, v. 24, PA2207, doi: 10.1029/2008PA001676.

Breecker, D. O., Sharp, Z. D., and McFadden, L. D., 2009, Seasonal bias in the formation and stable isotopic composition of pedogenic carbonate in modern soils from central New Mexico, USA: Geological Society of America Bulletin, v. 121, p. 630–640, doi: 10.1130/B26413.1.

Burgess, C. E., Pearson, P. N., Lear, C. H., Morgans, H. E. G., Handley, L., Pancost, R. D., and Schouten, S., 2008, Middle Eocene climate cyclicity in the southern Pacific: Implications for global ice volume: Geology, v. 36, p. 651–654, doi: 10.1130/G24762A.1.

Casson, S., and Gray, J. E., 2008, Influence of environmental factors on stomatal development: New Phytologist, v. 178, p. 9–23, doi: 10.1111/j.1469-8137.2007.02351.x.

Cerling, T. E., 1992, Use of carbon isotopes in paleosols as an indicator of the $P(CO_2)$ of the paleoatmosphere: Global Biogeochemical Cycles, v. 6, p. 307–314, doi: 10.1029/92GB01102.

DeConto, R. M., and Pollard, D., 2003, Rapid Cenozoic glaciation of Antarctica induced by declining atmospheric CO_2: Nature, v. 421, p. 245–249, doi: 10.1038/nature01290.

DeConto, R. M., Pollard, D., Wilson, P. A., Pälike, H., Lear, C. H., and Pagani, M., 2008, Thresholds for Cenozoic bipolar glaciation: Nature, v. 455, p. 652–656, doi: 10.1038/nature07337.

Edgar, K. M., Wilson, P. A., Sexton, P. F., and Suganuma, Y., 2007, No extreme bipolar glaciation during the main Eocene calcite compensation shift: Nature, v. 448, p. 908–911, doi: 10.1038/nature06053.

Ehrmann, W. U., and Mackensen, A., 1992, Sedimentological evidence for the formation of an East Antarctic ice sheet in Eocene/Oligocene time: Palaeogeography, Palaeoclimatology, Palaeoecology, v. 93, p. 85–112, doi: 10.1016/0031-0182(92)90185-8.

Ekart, D. D., Cerling, T. E., Montañez, I. P., and Tabor, N. J., 1999, A 400 million year carbon isotope record of pedogenic carbonate: implications for paleoatmospheric carbon dioxide: American Journal of Science, v. 299, p. 805–827, doi: 10.2475/ajs.299.10.805.

Eldrett, J. S., Harding, I. C., Wilson, P. A., Butler, E., and Roberts, A. P., 2007, Continental ice in Greenland during the Eocene and Oligocene: Nature, v. 446, p. 176–179, doi: 10.1038/nature05591.

Eldrett, J. S., Greenwood, D. R., Harding, I. C., and Huber, M., 2009, Increased seasonality through the Eocene to Oligocene transition in northern high latitudes: Nature, v. 459, p. 969–973, doi: 10.1038/nature08069.

Farquhar, G. D., Ehleringer, J. R., and Hubick, K. T., 1989, Carbon isotope discrimination and photosynthesis: Annual Review of Plant Physiology and Plant Molecular Biology, v. 40, p. 503–537, doi: 10.1146/annurev.pp.40.060189.002443.

Feng, W., and Yapp, C. J., 2009, Paleoenvironmental implications of concentration and $^{13}C/^{12}C$ ratios of $Fe(CO_3)OH$ in goethite from a mid-latitude Cenomanian laterite in southwestern Minnesota: Geochimica et Cosmochimica Acta, v. 73, p. 2559–2580, doi: 10.1016/j.gca.2009.02.004.

Fletcher, B. J., Brentnall, S. J., Anderson, C. W., Berner, R. A., and Beerling, D. J., 2008, Atmospheric carbon dioxide linked with Mesozoic and early Cenozoic climate change: Nature Geoscience, v. 1, p. 43–48, doi: 10.1038/ngeo.2007.29.

Franks, P. J., and Beerling, D. J., 2009, Maximum leaf conductance driven by CO_2 effects on stomatal size and density over geologic time: Proceedings of the National Academy of Sciences of the United States of America, v. 106, p. 10343–10347, doi: 10.1073/pnas.0904209106.

Freeman, K. H., and Hayes, J. M., 1992, Fractionation of carbon isotopes by phytoplankton and estimates of ancient CO_2 levels: Global Biogeochemical Cycles, v. 6, p. 185–198, doi: 10.1029/92GB00190.

Goslar, T., van der Knaap, W. O., Hicks, S., Andrič, M., Czernik, J., Goslar, E., Räsänen, S., and Hyötylä, H., 2005, Radiocarbon dating of modern peat profiles: pre- and post-bomb ^{14}C variations in the construction of age-depth models: Radiocarbon, v. 47, p. 115–134.

Gradstein, F. M., Ogg, J. G., and Smith, A. G., 2004, A Geologic Timescale 2004: Cambridge, United Kingom, Cambridge University Press, 589 p.

Gray, J. E., Holroyd, G. H., van der Lee, F. M., Bahrami, A. R., Sijmons, P. C., Woodward, F. I., Schuch, W., and Hetherington, A. M., 2000, The *HIC* signalling pathway links CO_2 perception to stomatal development: Nature, v. 408, p. 713–716, doi: 10.1038/35047071.

Greenwood, D. R., and Basinger, J. F., 1993, Stratigraphy and floristics of Eocene swamp forests from Axel Heiberg Island, Canadian Arctic Archipelago: Canadian Journal of Earth Science, v. 30, p. 1914–1923, doi: 10.1139/e93-169.

Greenwood, D. R., Scarr, M. J., and Christophel, D. C., 2003, Leaf stomatal frequency in the Australian tropical rainforest tree *Neolitsea dealbata* (Lauraceae) as a proxy measure of atmospheric pCO_2: Palaeogeography, Palaeoclimatology, Palaeoecology, v. 196, p. 375–393, doi: 10.1016/S0031-0182(03)00465-6.

Hetherington, A. M., and Woodward, F. I., 2003, The role of stomata in sensing and driving environmental change: Nature, v. 424, p. 901–908, doi: 10.1038/nature01843.

IPCC, 2007, Climate Change 2007: The Physical Science Basis, Contribution of Working Group I to the Fourth Assessment Report of the Intergovernmental Panel on Climate Change, *in* Solomon, S., Qin, D., Manning, M., Chen, Z., Marquis, M., Averyt, K. B., Tignor, M., and Miller, H. L., editors: Cambridge, Cambridge University Press, 996 p.

Ivany, L. C., Lohmann, K. C., Hasiuk, F., Blake, D. B., Glass, A., Aronson, R. B., and Moody, R. M., 2008, Eocene climate record of a high southern latitude continental shelf: Seymour Island, Antarctica: The Geological Society of America Bulletin, v. 120, p. 659–678, doi: 10.1130/B26269.1.

Jagniecki, E., Lowenstein, T. K., and Jenkins, D., 2010, Sodium carbonates: temperature and pCO_2 indicators for ancient and modern alkaline saline lakes: Geological Society of America Abstracts with Programs, v. 42(5), p. 404 (Paper No. 165-2).

Keeling, R. F., Piper, S. C., Bollenbacher, A. F., and Walker, J. S., 2009, Atmospheric CO_2 records from sites in the SIO air sampling network, http://cdiac.ornl.gov.

Kleidon, A., 2007, Optimized stomatal conductance and the climate sensitivity to carbon dioxide: Geophysical Research Letters, v. 34, L14709, doi: 10.1029/2007GL030342, p. 1–4.

Klochko, K., Kaufman, A. J., Yao, W. S., Byrne, R. H., and Tossell, J. A., 2006, Experimental measurement of boron isotope fractionation in seawater: Earth and Planetary Science Letters, v. 248, p. 276–285, doi: 10.1016/j.epsl.2006.05.034.

Klochko, K., Cody, G. D., Tossell, J. A., Dera, P., and Kaufman, A. J., 2009, Re-evaluating boron speciation in biogenic calcite and aragonite using ^{11}B MAS NMR: Geochimica et Cosmochimica Acta, v. 73, p. 1890–1900, doi: 10.1016/j.gca.2009.01.002.

Koch, P. L., Zachos, J. C., and Gingerich, P. D., 1992, Correlation between isotope records in marine and continental carbon reservoirs near the Palaeocene/Eocene boundary: Nature, v. 358, p. 319–322, doi: 10.1038/358319a0.

Kojima, S., Sweda, T., LePage, B. A., and Basinger, J. F., 1998, A new method to estimate accumulation rates of lignites in the Eocene Buchanan Lake Formation, Canadian Arctic: Palaeogeography, Palaeoclimatology, Palaeoecology, v. 141, p. 115–122, doi: 10.1016/S0031-0182(98)00011-X.

Konrad, W., Roth-Nebelsick, A., and Grein, M., 2008, Modelling of stomatal density response to atmospheric CO_2: Journal of Theoretical Biology, v. 253, p. 638–658, doi: 10.1016/j.jtbi.2008.03.032.

Kouwenberg, L. L. R., McElwain, J. C., Kurschner, W. M., Wagner, F., Beerling, D. J., Mayle, F. E., and Visscher, H., 2003, Stomatal frequency adjustment of four conifer species to historical changes in atmospheric CO_2: American Journal of Botany, v. 90, p. 610–619, doi: 10.3732/ajb.90.4.610.

Kürschner, W. M., 1997, The anatomical diversity of recent and fossil leaves of the durmast oak (*Quercus petraea* Lieblein/*Q. pseudocastanea* Goeppert)—implications for their use as biosensors of palaeoatmospheric CO_2 levels: Review of Palaeobotany and Palynology, v. 96, p. 1–30, doi: 10.1016/S0034-6667(96)00051-6.

Kürschner, W. M., van der Burgh, J., Visscher, H., and Dilcher, D. L., 1996, Oak leaves as biosensors of late Neogene and early Pleistocene paleoatmospheric CO_2 concentrations: Marine Micropaleontology, v. 27, p. 299–312, doi: 10.1016/0377-8398(95)00067-4.

Kürschner, W. M., Wagner, F., Dilcher, D. L., and Visscher, H., 2001, Using fossil leaves for the reconstruction of Cenozoic paleoatmospheric CO_2 concentrations, *in* Gerhard, L. C., Harrison, W. E., and Hanson, B. M., editors, Geological Perspectives of Global Climate Change: Tulsa, The American Association of Petroleum Geologists, p. 169–189.

Kürschner, W. M., Kvacek, Z., and Dilcher, D. L., 2008, The impact of Miocene atmospheric carbon dioxide fluctuations on climate and the evolution of terrestrial ecosystems: Proceedings of the National Academy of Sciences of the United States of America, v. 105, p. 449–453, doi: 10.1073/pnas.0708588105.

Lake, J. A., Quick, W. P., Beerling, D. J., and Woodward, F. I., 2001, Plant Development: Signals from mature to new leaves: Nature, v. 411, p. 154, doi: 10.1038/35075660.

Lake, J. A., Woodward, F. I., and Quick, W. P., 2002, Long-distance CO_2 signalling in plants: Journal of Experimental Botany, v. 53, p. 183–193, doi: 10.1093/jexbot/53.367.183.

Lemarchand, D., Gaillardet, J., Lewin, É., and Allègre, C. J., 2000, The influence of rivers on marine boron isotopes and implications for reconstructing past ocean pH: Nature, v. 408, p. 951–954, doi: 10.1038/35050058.

LePage, B. A., Yang, H., and Matsumoto, M., 2005, The evolution and biogeographic history of *Metasequoia, in* LePage, B. A., Williams, C. J., and Yang, H., editors, The Geobiology and Ecology of *Metasequoia:* Dordrecht, The Netherlands, Springer, Topics in Geobiology, v. 22, p. 3–114, doi: 10.1007/1-4020-2764-8_1.

Liu, C. Y.-S., and Basinger, J. F., 2009, *Metasequoia* Hu et Cheng (Cupressaceae) from the Eocene of Axel Heiberg Island, Canadian High Arctic: Palaeontographica Abteilung B, v. 282, p. 69–97.

Lowenstein, T. K., and Demicco, R. V., 2006, Elevated Eocene atmospheric CO_2 and its subsequent decline: Science, v. 313, p. 1928, doi: 10.1126/science.1129555.

Lloyd, A. H., 2005, Ecological histories from Alaskan tree lines provide insight into future change: Ecology, v. 86, p. 1687–1695, doi: 10.1890/03-0786.

McElwain, J. C., Mayle, F. E., and Beerling, D. J., 2002, Stomatal evidence for a decline in atmospheric CO_2 concentration during the Younder Dryas stadial: a comparison with Antarctic ice core records: Journal of Quaternary Science, v. 17, p. 21–29, doi: 10.1002/jqs.664.

Nordt, L., Atchley, S., and Dworkin, S. I., 2002, Paleosol barometer indicates extreme fluctuations in atmospheric CO_2 across the Cretaceous-Tertiary boundary: Geology, v. 30, p. 703–706, doi: 10.1130/0091-7613(2002)030<0703:PBIEFI>2.0.CO;2.

——— 2003, Terrestrial evidence for two greenhouse events in the latest Cretaceous: GSA Today, v. 13 (12), p. 4–9, doi: 10.1130/1052-5173(2003)013<4:TEFTGE>2.0.CO;2.

Pagani, M., Lemarchand, D., Spivack, A., and Gaillardet, J., 2005a, A critical evaluation of the boron isotope-*p*H proxy: The accuracy of ancient ocean *p*H estimates: Geochimica et Cosmochimica Acta, v. 69, p. 953–961, doi: 10.1016/j.gca.2004.07.029.

Pagani, M., Zachos, J. C., Freeman, K. H., Tipple, B., and Bohaty, S., 2005b, Marked decline in atmospheric carbon dioxide concentrations during the Paleogene: Science, v. 309, p. 600–603, doi: 10.1126/science.1110063.

Pearson, P. N., Foster, G. L., and Wade, B. S., 2009, Atmospheric carbon dioxide through the Eocene-Oligocene climate transition: Nature, v. 461, p. 1110–1113, doi: 10.1038/nature08447.

Peters, S. E., Carlson, A. E., Kelly, D. C., and Gingerich, P. D., 2010, Large-scale glaciation and deglaciation of Antarctica during the Late Eocene: Geology, v. 38, p. 723–726, doi: 10.1130/G31068.1.

Pollard, D., and DeConto, R. M., 2005, Hysteresis in Cenozoic Antarctic ice-sheet variations: Global and Planetary Change, v. 45, p. 9–21, doi: 10.1016/j.gloplacha.2004.09.011.

Retallack, G. J., 2001, A 300-million-year record of atmospheric carbon dioxide from fossil plant cuticles: Nature, v. 411, p. 287–290, doi: 10.1038/35077041.

——— 2009a, Greenhouse crises of the past 300 million years: Geological Society of America Bulletin, v. 121, p. 1441–1455, doi: 10.1130/B26341.1.

——— 2009b, Refining a pedogenic-carbonate CO_2 paleobarometer to quantify a middle Miocene greenhouse spike: Palaeogeography, Palaeoclimatology, Palaeoecology, v. 281, p. 57–65, doi: 10.1016/j.palaeo.2009.07.011.

Royer, D. L., 2001, Stomatal density and stomatal index as indicators of paleoatmospheric CO_2 concentration: Review of Palaeobotany and Palynology, v. 114, p. 1–28, doi: 10.1016/S0034-6667(00)00074-9.

——— 2003, Estimating latest Cretaceous and Tertiary atmospheric CO_2 from stomatal indices, *in* Wing, S. L., Gingerich, P. D., Schmitz, B., and Thomas, E., editors, Causes and Consequences of Globally Warm Climates in the Early Paleogene: Geological Society of America Special Paper 369, p. 79–93, doi: 10.1130/0-8137-2369-8.79.

——— 2006, CO_2-forced climate thresholds during the Phanerozoic: Geochimica et Cosmochimica Acta, v. 70, p. 5665–5675, doi: 10.1016/j.gca.2005.11.031.

Royer, D. L., Berner, R. A., and Beerling, D. J., 2001a, Phanerozoic atmospheric CO_2 change: evaluating geochemical and paleobiological approaches: Earth-Science Reviews, v. 54, p. 349–392, doi: 10.1016/S0012-8252(00)00042-8.

Royer, D. L., Wing, S. L., Beerling, D. J., Jolley, D. W., Koch, P. L., Hickey, L. J., and Berner, R. A., 2001b, Paleobotanical evidence for near present-day levels of atmospheric CO_2 during part of the Tertiary: Science, v. 292, p. 2310–2313, doi: 10.1126/science.292.5525.2310.

Rundgren, M., and Beerling, D., 1999, A Holocene CO_2 record from the stomatal index of sub-fossil *Salix herbacea* L. leaves from northern Sweden: The Holocene, v. 9, p. 509–513, doi: 10.1191/095968399677717287.

——— 2003, Fossil leaves: Effective bioindicators of ancient CO_2 levels?: Geochemistry Geophysics Geosystems, v. 4 (7), 1058, doi: 10.1029/2002GC000463, p. 1–5.

Rundgren, M., Björck, S., and Hammarlund, D., 2005, Last interglacial atmospheric CO_2 changes from stomatal index data and their relation to climate variations: Global and Planetary Change, v. 49, p. 47–62, doi: 10.1016/j.gloplacha.2005.04.002.

Rustad, J. R., and Zarzycki, P., 2008, Calculation of site-specific carbon-isotope fractionation in pedogenic oxide minerals: Proceedings of the National Academy of Sciences of the United States of America, v. 105, p. 10297–10301, doi: 10.1073/pnas.0801571105.

Sack, L., Cowan, P. D., Jaikumar, N., and Holbrook, N. M., 2003, The "hydrology" of leaves: co-ordination of structure and function in temperate woody species: Plant, Cell and Environment, v. 26, p. 1343–1356, doi: 10.1046/j.0016-8025.2003.01058.x.

Salisbury, E. J., 1927, On the causes and ecological significance of stomatal frequency, with special reference to the woodland flora: Philosophical Transactions of the Royal Society of London B, v. 216, p. 1–65, doi: 10.1098/rstb.1928.0001.

Sinha, A., and Stott, L. D., 1994, New atmospheric pCO_2 estimates from paleosols during the late Paleocene/early Eocene global warming interval: Global and Planetary Change, v. 9, p. 297–307, doi: 10.1016/0921-8181(94)00010-7.

Smith, R. Y., Greenwood, D. R., and Basinger, J. F., 2010, Estimating paleoatmospheric pCO_2 during the Early Eocene Climatic Optimum from stomatal frequency of *Ginkgo,* Okanagan Highlands, British Columbia, Canada: Palaeogeography, Palaeoclimatology, Palaeoecology, v. 293, p. 120–131, doi: 10.1016/j.palaeo.2010.05.006.

St. John, K., 2008, Cenozoic ice-rafting history of the central Arctic Ocean: Terrigenous sands on the Lomonosov Ridge: Paleoceanography, v. 22, PA1S05, doi: 10.1029/2007PA001483.

Stickley, C. E., St. John, K., Koç, N., Jordan, R. W., Passchier, S., Pearce, R. B., and Kearns, L. E., 2009, Evidence for middle Eocene Arctic sea ice from diatoms and ice-rafted debris: Nature, v. 460, p. 376–379, doi: 10.1038/nature08163.

Stott, L. D., 1992, Higher temperatures and lower oceanic pCO_2: A climate enigma at the end of the Paleocene Epoch: Paleoceanography, v. 7, p. 395–404, doi: 10.1029/92PA01183.
Sturm, M., Racine, C., and Tape, K., 2001, Climate change: Increasing shrub abundance in the Arctic: Nature, v. 411, p. 546–547, doi: 10.1038/35079180.
Sun, B., Dilcher, D. L., Beerling, D. J., Zhang, C., Yan, D., and Kowalski, E., 2003, Variation in *Ginkgo biloba* L. leaf characters across a climatic gradient in China: Proceedings of the National Academy of Sciences of the United States of America, v. 100, p. 7141–7146, doi: 10.1073/pnas.1232419100.
Tabor, N. J., and Yapp, C. J., 2005, Coexisting goethite and gibbsite from a high-paleolatitude (55 °N) Late Paleocene laterite: Concentration and $^{13}C/^{12}C$ ratios of occluded CO_2 and associated organic matter: Geochimica et Cosmochimica Acta, v. 69, p. 5495–5510, doi: 10.1016/j.gca.2005.07.017.
Torsvik, T. H., Van der Voo, R., Meert, J. G., Mosar, J., and Walderhaug, H. J., 2001, Reconstructions of the continents around the North Atlantic at about the 60th parallel: Earth and Planetary Science Letters, v. 187, p. 55–69, doi: 10.1016/S0012-821X(01)00284-9.
Torsvik, T. H., Müller, R. D., Van der Voo, R., Steinberger, B., and Gaina, C., 2008, Global plate motion frames: toward a unified model: Reviews of Geophysics, v. 46, RG3004, doi: 10.1029/2007RG000227.
Tripati, A., Backman, J., Elderfield, H., and Ferretti, P., 2005, Eocene bipolar glaciation associated with global carbon cycle changes: Nature, v. 436, p. 341–346, doi: 10.1038/nature03874.
Tripati, A. K., Eagle, R. A., Morton, A., Dowdeswell, J. A., Atkinson, K. L., Bahé, Y., Dawber, C. F., Khadun, E., Shaw, R. M. H., Shorttle, O., and Thanabalasundaram, L., 2008, Evidence for glaciation in the Northern Hemisphere back to 44 Ma from ice-rafted debris in the Greenland Sea: Earth and Planetary Science Letters, v. 265, p. 112–122, doi: 10.1016/j.epsl.2007.09.045.
Tripati, A. K., Roberts, C. D., and Eagle, R. A., 2009, Coupling of CO_2 and ice sheet stability over major climate transitions of the last 20 million years: Science, v. 326, p. 1394–1397, doi: 10.1126/science.1178296.
Vann, D. R., 2005, Physiological ecology of *Metasequoia glyptostroboides* Hu et Cheng, *in* LePage, B. A., Williams, C. J., and Yang, H., editors, The Geobiology and Ecology of *Metasequoia:* Dordrecht, The Netherlands, Springer, Topics in Geobiology, v. 22, p. 305–334, doi: 10.1007/1-4020-2764-8_10.
Westgate, J. A., Naeser, N. D., and Alloway, B., 2006, Fission-track dating, *in* Elias, S. A., editor, Encyclopedia of Quaternary Science: Amsterdam, Elsevier, v. 1, p. 651–672.
Wolfe, A. P., Edlund, M. B., Sweet, A. R., and Creighton, S. D., 2006, A first account of organelle preservation in Eocene nonmarine datoms: observations and paleobiological implications: Palaios, v. 21, p. 298–304, doi: 10.2110/palo.2005.p05-14e.
Woodward, F. I., and Bazzaz, F. A., 1988, The responses of stomatal density to CO_2 partial pressure: Journal of Experimental Botany, v. 39, p. 1771–1781, doi: 10.1093/jxb/39.12.1771.
Wynn, J. G., 2003, Towards a physically based model of CO_2-induced stomatal frequency response: New Phytologist, v. 157, p. 391–398, doi: 10.1046/j.1469-8137.2003.00702.x.
Yang, H., Huang, Y., Leng, Q., LePage, B. A., and Williams, C. J., 2005, Biomolecular preservation of Tertiary *Metasequoia* fossil *lagerstätten* revealed by comparative pyrolysis analysis: Review of Palaeobotany and Palynology, v. 134, p. 237–256, doi: 10.1016/j.revpalbo.2004.12.008.
Yapp, C. J., 2004, $Fe(CO_3)OH$ in goethite from a mid-latitude North American Oxisol: Estimate of atmospheric CO_2 concentration in the Early Eocene "climatic optimum": Geochimica et Cosmochimica Acta, v. 68, p. 935–947, doi: 10.1016/j.gca.2003.09.002.
Yapp, C. J., and Poths, H., 1996, Carbon isotopes in continental weathering environments and variations in ancient atmospheric CO_2 pressure: Earth and Planetary Science Letters, v. 137, p. 71–82, doi: 10.1016/0012-821X(95)00213-V.
Zachos, J., Pagani, M., Sloan, L., Thomas, E., and Billups, K., 2001, Trends, rhythms, and aberrations in global climate 65 Ma to present: Science, v. 292, p. 686–693, doi: 10.1126/science.1059412.